CHEMISTRY OF MATERIALS

Article

pubs.acs.org/cm

Facile and Scalable One-Step Method for Amination of Graphene Using Leuckart Reaction

Héctor Aguilar-Bolados,*[,†] Daniela Vargas-Astudillo,[‡] Mehrdad Yazdani-Pedram,*[,‡] Gabriela Acosta-Villavicencio,[‡] Pablo Fuentealba,[‡] Ahirton Contreras-Cid,[‡] Raquel Verdejo,[§] and Miguel A. López-Manchado[§]

[†]Facultad de Ciencias Físicas y Matemáticas, Universidad de Chile, Beauchef 850, 8380492 Santiago, Chile

[‡]Facultad de Ciencias Químicas y Farmacéuticas, Universidad de Chile, S. Livingstone 1007, 8380492 Santiago, Chile

[§]Instituto de Ciencia y Tecnología de Polímeros, ICTP-CSIC, Juan de la Cierva, 3, 28006-Madrid, Spain

ABSTRACT: A very simple method of reductive amination, based on the Leuckart reaction, is reported. This method enables not only the reduction of graphite oxide but also results in reduced graphene oxide functionalized with amine groups, where the amination degree is 3.2 at. % as determined by XPS. The dominant nitrogen functional group was primary amine, but pyridines and lactam groups were also observed. It was found that the amino-functionalized reduced graphene oxide is a semi-metallic material because of the lack of band gap, unlike the graphite oxide that presented a band gap of 2.16 eV.

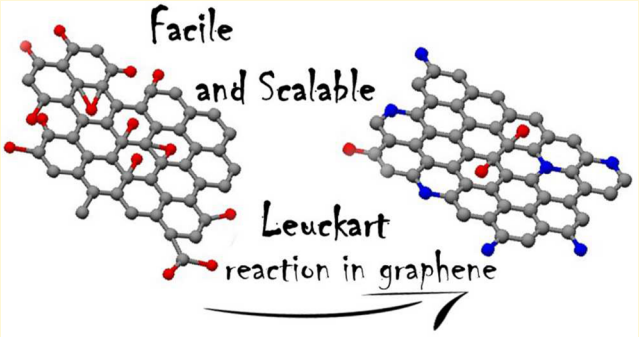

INTRODUCTION

The development of appropriate methods to modify carbon allotropes, such as graphene, has sparked scientific interest over the past decade. The graphene was isolated for the first time by mechanical exfoliation (repeated peeling) of small mesas of highly oriented pyrolytic graphite.[1] Graphene is a two-dimensional (2D) network of sp^2 carbon atoms arranged in a honeycomb lattice[2] and is the building block of other carbon allotropes, such as carbon nanotubes, graphite, graphene nanoribbons, and fullerenes.[3] Interest in graphene has arisen due to its unique properties.[4−9] The excellent electronic properties of graphene are defined by its band structure, having the valence and conduction bands in contact but not overlapping.[6,9−11]

The method of mechanical exfoliation of highly oriented pyrolytic graphite is not useful for producing large quantities of graphene.[1] Therefore, several alternative methods have been proposed and have been divided into two groups, bottom-up and top-down methods. Bottom-up mainly refers to those methods using chemical vapor deposition.[12,13] Meanwhile, the top-down methods consist of obtaining graphene from graphite via its oxidation and subsequent chemical or thermal reduction.[14] Graphite oxide (GO) is produced in the presence of strong acids and oxidants, following well-known methods: Brodie,[15] Staudenmaier,[16] Hofmann,[17] Hummers,[18] and Tour.[19] Jankovský et al.[20] have thoroughly studied these GOs and their corresponding chemically or thermally reduced GOs. This work indicates that all these methods produce GOs that contain reactive oxygen functional groups, such as carbonyl, carboxyl, and ether.[20] Among the oxidation protocols, the most studied is Hummers' method, since it provides the highest oxidation degree. However, it also produces severe damage on the graphitic structure as compared to Brodie's method.[21] The carbon−oxygen moieties of GOs can subsequently be removed to produce graphene, termed reduced graphene oxide (rGO), with restored surface morphology and electrical, thermal, and mechanical properties.[23] The chemical methods used for the reduction of graphite oxide can be cumbersome or can require the use of dangerous chemical reagents, such as hydrazine, its derivatives, or $NaBH_4$.[14,24] Here, we advance a new, easily scalable reduction protocol that directly results in amino-functionalized reduced graphene oxide (rGO-Am).

Amine functionalization of graphene has been pursued for various applications in energy storage,[25,26] as drug-delivery vehicles,[27] transparent electrodes for polymer solar cells,[28] sensors for aqueous contaminants,[29] or biomolecules[30] and composites.[31,32] The majority of these studies have been carried out directly on the graphite oxide, using different reactants and extending the initial work by Bourlinos et al.[33] However, this strategy retains the insulating character of GO. Amination of graphene or reduced graphene oxide has received less consideration since specific equipment, hazardous chemicals, or a large number of steps are required.[25,26,31,34,35] For instance, Bittolo Bon et al.[34] reported the amination of thermally reduced graphene oxide (TRGO) via plasma activation. They first covalently attached fluorine to the TRGO sheets by plasma-assisted decomposition of CF_4 gas and then exposed

Received: April 7, 2017
Revised: July 27, 2017
Published: July 28, 2017

DOI: 10.1021/acs.chemmater.7b01438
Chem. Mater. 2017, 29, 6698−6705

this material to butylamine at room temperature. The resulting material was used to develop transparent electrodes for polymer solar cells with improved power conversion efficiencies compared to nonfunctionalized graphene oxide.[28] Similarly, Zhang et al.[31] reported the preparation of amino-functionalized graphene oxide using the Hoffman rearrangement, which consists of the change of amide into amine groups. This method allows one to reach a nitrogen content of around 4 at. %. However, this work required several steps and the use of dangerous reactants, such as thionyl chloride. Other authors have produced N-doped graphene using hydrothermal procedures.[35−43] The hydrothermal method generally consists of the simultaneous reduction and functionalization of GO, using reagents such as ammonia[35−38] urea[39−41] and other nitrogenous compounds,[38,42,43] that leads to graphene layers containing pyridinic, pyrrolic and graphitic N.[36] However, these amination protocols entailed long reaction times, 10 h, and the use of an autoclave at high temperatures, around 180 °C. On the other hand, a common method for the amination of aromatic compounds is the Leuckart reaction.[44−47] The Leuckart reaction is a very simple type of reductive amination, which involves the conversion of a carbonyl group of an aldehyde or a ketone to an amine group (Figure 1). Hence, this

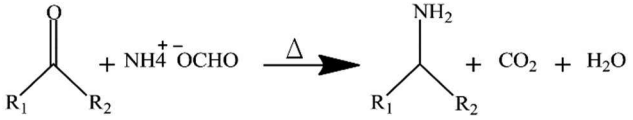

Figure 1. Reductive amination reaction by using ammonium formate.

reaction could be suitable for the reduction of graphite oxide. This work reports, for the first time, the use of the Leuckart reaction for the reduction of GO with the aim of obtaining aminated graphene.

EXPERIMENTAL SECTIONS

Synthesis of Graphite Oxide. GO was prepared using the method reported by Brodie.[15] The oxidation reaction was carried out by adding 5 g of graphite to 100 mL of fuming nitric acid (98%, Sigma-Aldrich, Germany) in a reactor at 0 °C. Then, 40 g of potassium chlorate was slowly added and left to react for 22 h. After, the mixture was poured into 500 mL of cold distilled water. This suspension was centrifuged and washed several times until the pH was 4.5. Finally, sediment GO was dried at 70 °C for 12 h. The mass of the product was 6.03 g.

Reductive Amination Reaction. Amino-functionalized reduced graphene oxide was obtained by using the Leuckart reaction. First, 5 g of graphite oxide and 25 g of ammonium formate were mixed and pulverized in a porcelain mortar. Then, this mixture was placed in a round-bottom flask fitted with a condenser. The temperature of the reaction was raised to 135 °C by using a heating mantle and left to react for 4 h. Afterward, the content of the flask was recovered using distilled water. This suspension was centrifuged and washed with abundant distilled water to pH 7. Finally, the product was dried at 70 °C for 12 h. The mass of the product was 3.55 g.

Characterization. The graphene materials were characterized by infrared spectroscopy (FTIR), using a PerkinElmer Spectrum Two FTIR spectrometer (Massachusetts, USA) and by Raman spectroscopy using a Jobin Yvon Horiba (HR800) microspectrometer equipped with a 532 nm wavelength laser and 0.02 cm^{-1} resolution. The spectra were recorded from 0 to 4000 cm^{-1}. The chemical composition of different graphene materials was studied by means of chemical binding energy of the elements, through X-ray photoelectron spectroscopy technique (XPS), using a PerkinElmer XPS−Auger spectrometer, model PHI 1257. This spectrometer includes an ultrahigh vacuum chamber, a hemispheric electron energy analyzer, and an X-ray source with Kα radiation unfiltered from an Al ($h\nu$ = 1486.6 eV) anode. The measurements were performed at 400 W and emission angle of 70° in order to obtain information from the deep surface. Thermogravimetric (TGA) analyses were carried out in the 25−800 °C temperature range, using a Netzsch thermogravimetric analyzer model Iris TG 209 F1 in nitrogen atmosphere at 5 °C/min heating rate.

The Kaiser test was used to determine the content of amino functional groups in rGO-Am. The methodology consisted of the addition of 10 mL of ninhydrin solution with different concentrations (0.746−22.4 mM) to a fixed amount of rGO-Am (0.5 g). It is expected a threshold concentration would be observed. The ninhydrin solutions will show similar absorbance above this threshold concentration, since amino groups present in rGO-Am will limit the numbers of ninhydrin molecules that can react. The rGO-Am suspensions in ninhydrin solutions were sonicated for 5 min, and then, the vials were placed in boiling water for 30 s. Then, the suspensions were filtered by using hydrophilic syringe filters (0.45 μm, Sartorius stedim SA, Germany). The resulting solutions were measured using a UV−vis spectrometer, model Cary 8454, Agilent, USA.

Likewise, graphitic materials were characterized by X-ray diffraction analysis using a Bruker diffractometer model D8 Advance (Massachusetts, USA) with a Cu Kα radiation source, wavelength λ = 0.154 nm, and power supply of 40 kV and 40 mA. The incident angle (2θ) was varied between 2° and 80°, and the scan rate was 0.02 deg/s. The interlayer distance (d_{00l}) of graphitic materials was determined by Bragg's law (eq 1).

$$d_{00l} = \lambda/2 \sin \theta_{00l} \quad (1)$$

where d_{00l} is the interlayer distance and θ_{00l} is the reflection angle of the reflection plane, where 00l is an integer number.

The morphology of the graphitic materials was studied using transmission electron microscope (TEM, JEOL 2000 EX-II operating at 160 keV). Both GO and rGO-Am were dispersed for 20 min in dimethylformamide (DMF) using an ultrasonication bath, and the solutions were then drop cast on standard holey carbon copper grids for TEM analysis.

Solid state spectra was recorded in a PerkinElmer Lambda 650 equipment coupled with an integration sphere that consists of Praying Mantis Diffuse Reflection Accessory and a "Sampling Kit", model DRP-SAP, Harrick Scientific Products, Inc. (New York, USA). Band gap value was estimated by extrapolation of the region of linearity of the Tauc plots, $(\alpha h\nu)^2$ vs $h\nu$, where α is the absorption coefficient.[48]

RESULTS AND DISCUSSION

FTIR spectroscopy (Figure 2) was used to establish qualitatively the nature of the surface groups of graphite,

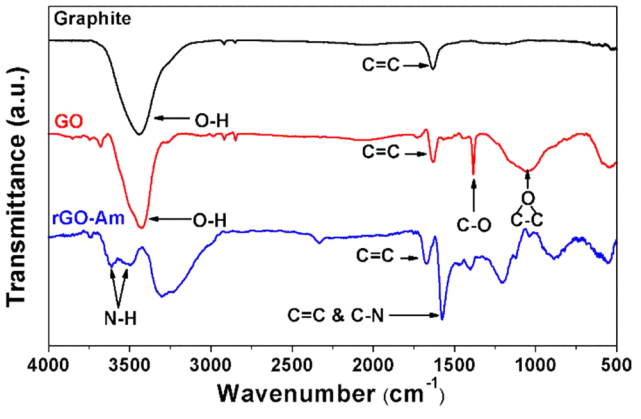

Figure 2. FTIR spectra of graphite, GO, and rGO-Am.

graphite oxide, and rGO-Am. The absorption band at 3470 cm^{-1} was assigned to the stretching vibration of the O−H bond of the hydroxyl groups present in graphite. The presence of this

DOI: 10.1021/acs.chemmater.7b01438
Chem. Mater. 2017, 29, 6698−6705

absorption band indicates a slight degree of oxidation. Another absorption band at 1632 cm^{-1}, observed for graphite, corresponds to the stretching vibration of C=C. FTIR spectrum of GO presents absorption bands corresponding to hydroxyl and C=C groups around 3470 and 1628 cm^{-1}, respectively. Moreover, as a result of the oxidation process, a band at 1728 cm^{-1} corresponding to ketone carbonyl groups is observed. Additionally, GO presents two absorption bands at 1387 and 1063 cm^{-1}, which correspond to stretching vibration modes of C−O bond.[49] Therefore, FTIR analysis shows that GO contains functional groups susceptible to the reductive amination reaction. After the aminated reduction, the FTIR spectrum of the product shows two new absorption bands at 3611 and 3496 cm^{-1} corresponding to the stretching of the N−H bond of primary amine. The broad absorption band observed around 3300 cm^{-1} could correspond to the stretching vibration of amide-A.[50] Additionally, as a result of the reductive amination reaction, the carbonyl absorption band of GO at 1628 cm^{-1} was significally decreased in rGO-Am. Furthermore, an intense absorption band appears at 1574 cm^{-1}, which could be attributed to conjugated double bonds present in the pyridine structure.[51] However, there is some controversy in the literature in the assignment of bands between 1500 and 1600 cm^{-1} for graphene materials. Several authors[52−55] have associated this band to the superposition of C=C and C=N vibrations for N-doped graphene materials produced by the hydrothermal process. By contrast, Navaee and Salami[56] have associated the band at 1550 cm^{-1} to N−H bending.

Figure 3 shows the Raman spectra of graphite, GO, and rGO-Am, where characteristic bands of graphitic materials are

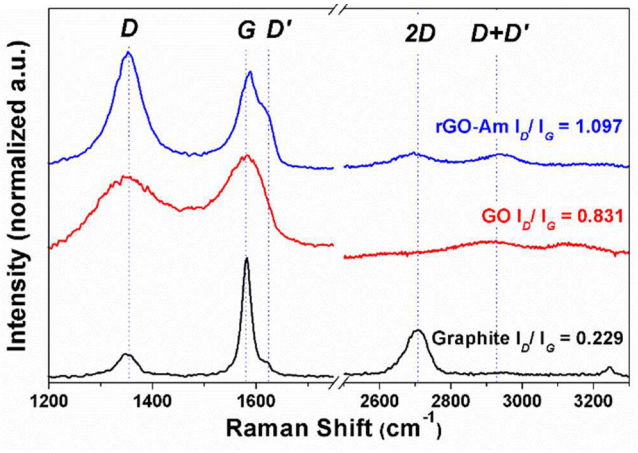

Figure 3. Raman spectra of graphite, GO, and rGO-Am.

observed. The G band appears around 1580 cm^{-1}, which corresponds to the first-order scattering of the E_{2g} phonon mode of sp^2 carbon atoms. The D band at ∼1350 cm^{-1} is associated with the breathing modes of six-atom rings and requires "defects" for its activation. Likewise, the D′ band, which appears around 1620 cm^{-1}, is associated with the breathing modes, since D and D′ are the result of an intervalley process of double resonance.[57] The band observed at 2700 cm^{-1} corresponds to an overtone of the D band and is termed 2D band. The band observed at 2920 cm^{-1} is a combination of the overtones of D and D′ bands. This band is called the D + D′ band.[57] The so-called defect density (I_D/I_G), which is the ratio of intensities of the D and G bands, is used to estimate the level of damage of graphene-based materials and the in-plane crystallite size (L_α).[58] The Raman data indicate a significant increase in disorder by comparing the GO (I_D/I_G = 0.83; L_α = 23.2 nm) and the rGO-Am (I_D/I_G = 1.10; L_α = 17.5 nm) with graphite (I_D/I_G = 0.23; L_α = 83.6 nm). This increase in the intensity ratio is commonly observed upon graphite oxidation,[57] and it is attributed to the structural changes resulting from the oxidation process and the presence of functional groups. rGO-Am presents an intense D′ band and two second-order bands (2D band and D + D′ band) of medium intensity. This could be attributed to nitrogen functional groups which play a role in the double resonant processes that occur in a phonon (D and D′ bands) and the double resonant processes that involves two phonons (2D and D + D′ bands). A similar Raman spectrum of aminated graphene was reported by Zhang et al.[31] Nitrogen functional groups, due to their nature, favor the occurrence of double resonant processes compared to oxygen functional groups. The presence of these second-order bands could suggest that nitrogen groups play a role in the sp^2 system. This assumption is supported by a theoretical study of N-doped graphene, where it is stated that the nitrogen atoms interact through sp^2 hybridization, since there is almost no distortion in the planar structure of graphene, but could break the symmetry of the graphene sublattices.[59]

The corresponding percentages of the atomic concentrations of carbon, oxygen, and nitrogen were quantitatively determined by X-ray photoelectron spectroscopy (XPS), analyzing the C 1s, O 1s, and N 1s regions. The percentage atomic concentrations in graphite were 91.8 at. % carbon and 8.2 at. % oxygen and in GO 73.9 at. % carbon and 26.1 at. % oxygen, and rGO-Am shows 89.0 at. % carbon, 3.2 at. % nitrogen, and 7.8 at. % oxygen. The oxygen content in GO (26.1 at. %) is three times that of graphite (8.2 at. %), which is in agreement with previous studies on graphite oxides produced via Brodie's reaction.[34,60] The oxygen content of rGO-Am is significantly lower than that of GO, as the result of the reductive amination of GO. Moreover, it is observed that the nitrogen content of rGO-Am is 3.2 at. %, which is consistent with its lower oxygen content. Such nitrogen content is slightly lower than the 4 at. % reported by Zhang et al.,[31] which could be due to differences in the initial oxygen content in the GO. Finally, although the hydrothermal methods have reported higher values of nitrogen functionalization, around 10 at. %,[39] these protocols are lengthy and difficult to carry out or to scale.

Figure 4 shows the C 1s signals, between 280 and 296 eV binding energy, of graphite, GO, and rGO-Am. The contributions of the functional groups to these C 1s signals were calculated using the *Shirley* model fit. The deconvolution of the C 1s peak of graphite shows the contributions of sp^2/sp^3 and oxygenated functional groups such as hydroxyls and ethers (C−O and C−O−C, respectively). As expected, after the oxidation, the GO has an intense C−O band, greater than that observed for graphite, indicating the increase of oxygenated functional groups.

This contribution of oxygenated groups decreases and a new N 1s signal appears after the reductive amination reaction. The curve fitting of N 1s signal indicates the presence of three bands at 398.5, 400.0, and 401.7 eV. The most intense band (400.0 eV) corresponds to amine and amide groups.[61] This band is consistent with the absorption band that appears around 3600 cm^{-1} in the FTIR spectrum of rGO-Am, which was attributed to amine groups. The bands observed at 398.5 and 401.7 eV are associated with pyridine and protonated lactam groups, respectively. This could indicate that the

DOI: 10.1021/acs.chemmater.7b01438
Chem. Mater. 2017, 29, 6698−6705

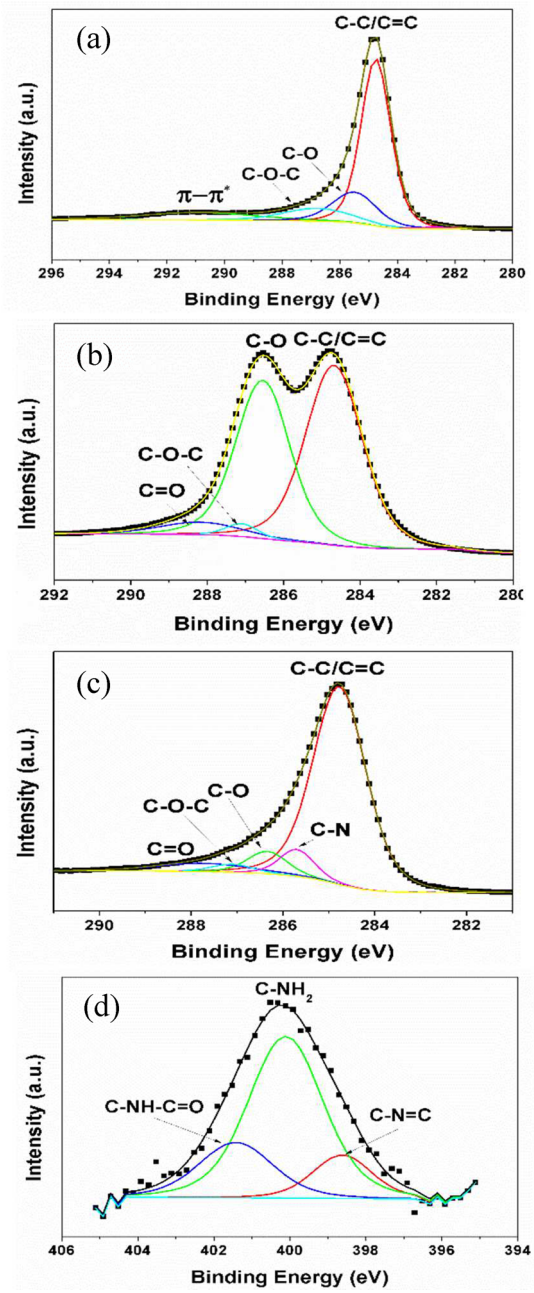

Figure 4. Contributions of functional groups of C 1s signals obtained from analysis of X-ray photoelectron spectroscopy (XPS) of graphite (a), GO (b), and rGO-Am (c) and contributions of functional groups of N 1s signal of rGO-Am (d).

reductive amination reaction produces functionalized graphene with amine groups and favors the formation of pyridines and lactams along the hexagonal lattice of graphene at later stages of the reaction.[25,26,31] Hence, the absence of high pressure in Leuckart's reaction could be favoring the formation of amine groups as compared to previous hydrothermal reactions using nitrogen compounds.[37−41]

Thermogravimetric analyses of graphite, GO, and rGO-Am were carried out under nitrogen atmosphere. The thermal decomposition of the materials presents significant differences (Figure 5). As expected, graphite does not show mass loss in the analyzed temperature range which is attributed to the high thermal stability of this material.[62] Meanwhile, GO presents an abrupt mass loss of nearly 83% at ∼270 °C. This loss is

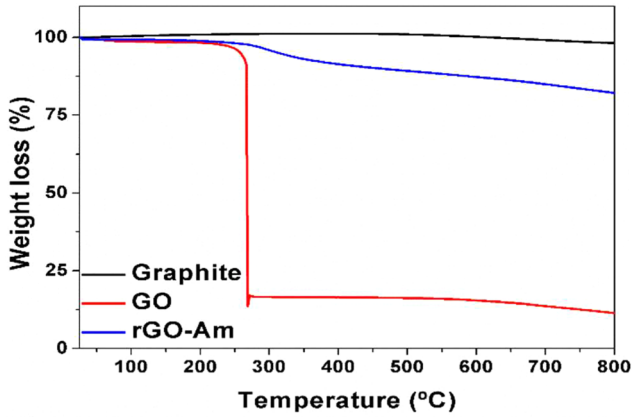

Figure 5. Thermogravimetric analysis of graphite, GO, and rGO-Am.

attributed to the concomitant decomposition of the oxygenated groups and the thermal blasting of GO.[60] In the case of rGO-Am, a gradual and slight mass loss between 250 and 400 °C is observed, which could correspond to the thermal decomposition of both nitrogen and oxygen groups. At 400 °C, the mass loss reaches 9%, which suggests that the oxygenated groups present in rGO-Am are less than those present in GO. This fact could indicate that the reductive amination successfully accomplishes the reduction of GO. Besides, mass loss at lower temperature to 200 °C was not observed. This observation is an important fact, because ammonium formate presents a boiling point at 180 °C and, hence, we can dismiss the presence of ammonium formate residues.

The presence of functional groups, such as amine, can also be identified by a chemical test. Frequently, amines are detected either by the Hinsberg test, the Kaiser test, or copper complex formation. It is not possible to use Hinsberg test or copper complex formation for materials such as rGO-Am, since the amine functions are linked to the graphene sheets and, hence, it is difficult to obtain precipitates or complexes. The Kaiser test is useful to detect amino acids and to differentiate them from amines.[63] The Kaiser test requires the use of ninhydrin as indicator. Ninhydrin yields a blue-violet color (Ruhemann's purple) in the presence of α-amino acids or orange, yellow or red in the presence of amines and amino acids that do not possess α-amino groups. Ruhemann's purple dye has a maximum absorption at 570 nm, while the yellow dye has a maximum absorption at 440 nm and is related to the formation of "imino acids".[64] Figure 6a shows the resulting filtered solutions of the Kaiser test. The more concentrated solutions show a yellow color, which could be due to the formation of imino acids. Hence, the values of absorbance at 440 nm of these solutions were registered. As expected, similar values of absorbance were found for samples with ninhydrin concentration between 7.46 and 22.4 mM (Figure 6b). This result indicates that a threshold amount of available amine groups exists to react with ninhydrin at 7.46 mM. Therefore, it is possible to assume that the rGO-Am presents 7.46 μmol of amine groups per 0.5 g of rGO-Am. The lack of Ruhemann's purple color can be attributed to the fact that rGO-Am is a complex system and it is not possible to differentiate between primary or secondary amines, since some primary amines such as *tert*-butyl amine show a yellow color (Figure 6c). Nevertheless, even with the positive result, it is important to remark that the Kaiser test is a useful and well-known procedure in molecular systems, where amine groups are

DOI: 10.1021/acs.chemmater.7b01438
Chem. Mater. 2017, 29, 6698−6705

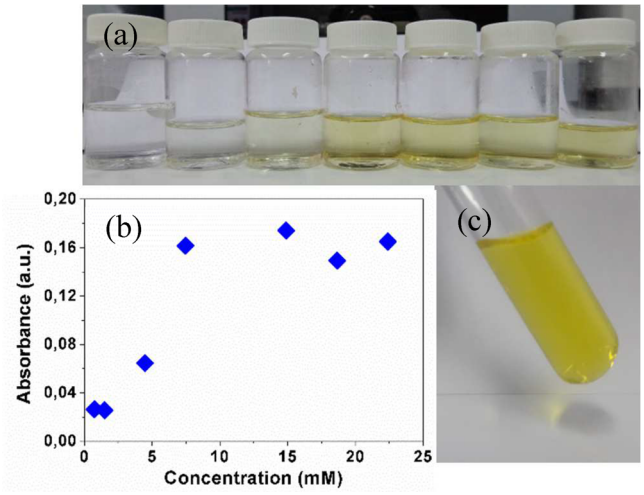

Figure 6. Images of vials containing the resulting solutions after Kaiser test performed on rGO-Am (a); UV absorbance values at 400 nm of ninhydrin solutions after performing the Kaiser test (b); result of Kaiser test performed on *tert*-butyl amine (c).

much more reactive than in a graphitic material, a much more complex system that does not allow the clear quantification of the amine groups.

The bulk crystalline structure of the materials was determined by X-ray diffraction (Figure 7). The characteristic

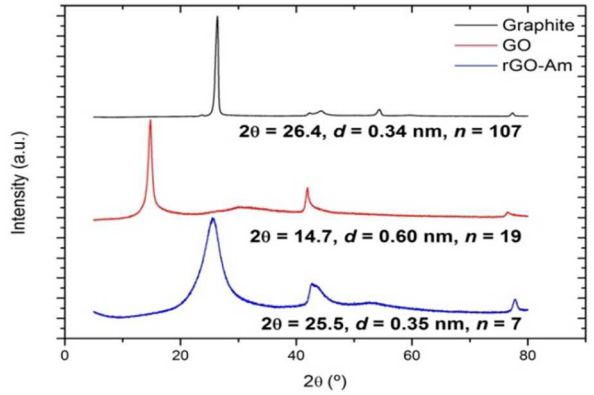

Figure 7. X-ray diffraction patterns of graphite, GO, and rGO-Am, with their diffraction angles 2θ, interlayer distances d, and number of layers.

peak of graphite is observed at $2\theta = 26°$, which corresponds to the (002) reflection. Upon oxidation, this graphitic peak appears at $2\theta = 15°$, characteristic of Brodie's oxidation protocol.[21,22] Moreover, rGO-Am shows a peak corresponding to (002) reflection around $2\theta = 26°$. This peak is wider and less intense than that exhibited by graphite, ascribed to the loss of the long-range order of the crystalline structure resulting from the oxidation and subsequent reductive amination reaction. Figure 7 also presents the values of reflection degree (θ_{002}), interlayer distance (d_{002}) determined by the Bragg's law, and the number of graphene layers, calculated using the Debye–Scherrer equation and fitting the (002) reflection to a Lorentzian curve.[65] This procedure, compared to AFM estimates, provides a value of the upper bound on the number of layers but should ensure that the materials are not altered during sample preparation. The observed greater interlayer distance of GO, 0.64 nm, compared to that of graphite, 0.34 nm, is explained by the presence of oxygenated functional groups in the GO structure.[60] rGO-Am exhibits a value of interlayer distance of 0.35 nm, similar to that of graphite. The decrease in the interlayer distance of rGO-Am with respect to GO indicates the elimination of oxygenated functional groups. The oxidation protocol drastically reduces the number of layers from ~107, for the parent graphite, to ~19, for GO. A similar number of layers has been reported by Kaniyoor et al.[65] The final material is composed of stacks of maximum ~7 layers. This fact indicates that the reductive amination of graphene oxide can be useful for the production of few-layer graphene materials.

Representative TEM images show the morphologies of GO and rGO-Am (Figure 8), which are largely composed of

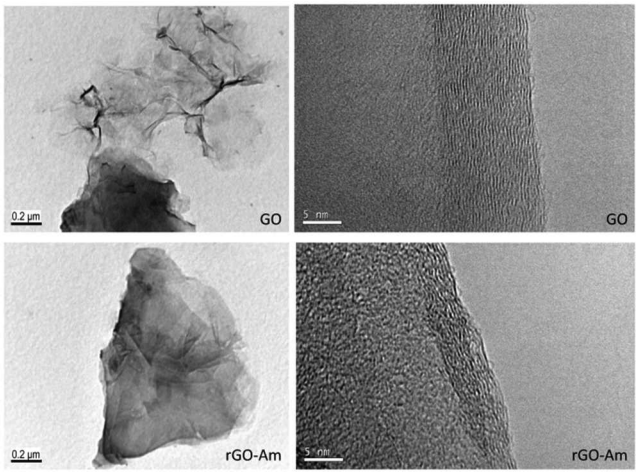

Figure 8. HRTEM images of GO and rGO-Am.

few-layer sheets' particles with lamellar morphology. The number of these stacked layers is significantly higher for GO, consistent with the XRD analysis. Some exfoliated and wrinkled sheets are also visible in the GO sample, due to the ultrasonication process in DMF. The oxygenated groups on the GO are known to result in stable suspensions in polar solvents facilitating the exfoliation of GO into graphene oxide.[66]

The band gap of these materials was calculated from the corresponding Tauc plots (Figure 9). Graphene is described as

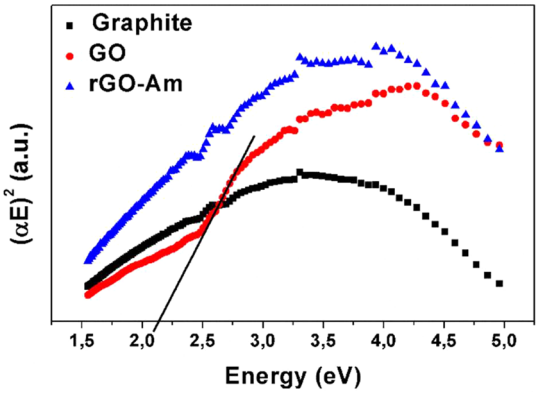

Figure 9. Tauc plots of studied phases of graphite, GO, and rGO-Am.

a semi-metal, since the valence and conduction bands are in contact but do not overlap.[6,9−11] The π electrons are those

DOI: 10.1021/acs.chemmater.7b01438
Chem. Mater. 2017, 29, 6698−6705

responsible for the electronic properties at low energies, whereas the σ electrons form energy bands far away from the Fermi energy and do not play a part in the conductivity.[67] Therefore, since the oxidation reaction is on the double bonds of graphene, the band structure suffers a modification. Tauc plot of GO shows an absorption edge close to 2.16 eV, probing that the conduction and valence bands are no longer in contact. This value is lower than values reported for other GOs obtained by Hummers' method (band gaps from 2.9 to 4.4 eV).[68] These differences are expected, since different oxidation degrees are obtained using different oxidation procedures.[42] On the other hand, after reduction of GO by Leuckart reaction, again no absorption edge is observed. It is known that GO recovers the sp^2 configuration when subjected to reduction reactions.[69] Therefore, the conjugated structure of GO is restored as well as its conductor character.

The results so far discussed have shown the successful reduction and amination of graphite oxide using the Leuckart reaction. Usually, this reaction is performed using ammonium formate or formamide in the presence of formic acid.[70] This is because formic acid maintains a slightly acidic medium, which traps ammonia and could diminish the aldol-type side reactions.[71] The slightly acid nature of GO could be a factor that favors the occurrence of the reductive amination reaction. Furthermore, the amine functional groups could react in later stages of the reaction with oxygenated functional groups, such as carboxylic acids or alcohols, present in the graphene, to yield pyridines and lactams groups. Figure 10 shows a scheme of a possible structure of rGO-Am based on the presence of pyridine and lactam-type groups observed by XPS analysis.

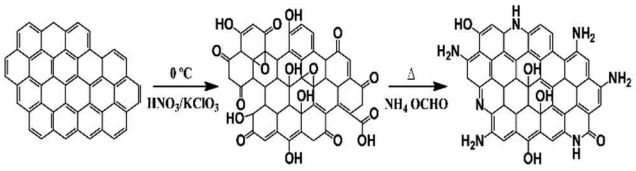

Figure 10. Scheme of the possible structure of GO and rGO-Am.

CONCLUSIONS

We have developed a novel approach, which is easy to scale up, for the production of amino-functionalized reduced graphene oxide using the Leuckart reaction. Both FTIR and XPS spectroscopy analyses indicate the presence of primary amino groups, pyridines, and lactam groups. In addition, the reductive amination alters the double resonant processes that occur in phonon (D and D′ bands) and the double resonant processes that involves two phonons (D and D + D′ bands). This could be related to the lack of a band gap in aminated graphene, which indicates its semi-metallic nature. rGO-Am presents morphological differences compared to both graphite and GO with a lower number of stacked layers and the in-plane crystallite size. Not only do these facts indicate that the Leuckart reaction is a very simple and effective approach to reduce graphite oxide, but also this reaction is a feasible and easy method to functionalize simultaneously graphene materials.

AUTHOR INFORMATION

Corresponding Authors

*(H.A.-B.) E-mail: haguilar@ciq.uchile.cl.
*(M.Y.-P.) E-mail: myazdani@ciq.uchile.cl.

ORCID

Héctor Aguilar-Bolados: 0000-0002-5927-9494

Author Contributions

H.A.-B., D.V.-A., M.Y.-P., G A.-V., P.F., A.C.-C., R.V., and M.A.L.-M. contributed equally to this work.

Funding

The authors declare no competing financial interest.

Notes

The authors declare no competing financial interest.

ACKNOWLEDGMENTS

This research was supported by the National Commission for Scientific and Technological Research (CONICYT), Chile, under Postdoctoral Fellowship No. 3170104 granted to H.A.-B.; the Vice Presidency of Research and Development (VID), Universidad de Chile, Chile, under Project Enlaces 2017 granted to M.Y.-P.; and the Spanish Ministry of Science and Innovation (MICINN), Spain, under Project MAT2013-48107-C3.

REFERENCES

(1) Novoselov, K. S.; Geim, A. K.; Morozov, S. V.; Jiang, D.; Zhang, Y.; Dubonos, S. V.; Grigorieva, I. V.; Firsov, A. A. Electric Field Effect in Atomically Thin Carbon Films. *Science* **2004**, *306*, 666−669.
(2) Endo, M.; Strano, M. S.; Ajayan, P. M. Potential Applications of Carbon Nanotubes. In *Carbon Nanotubes: Advanced Topics in the Synthesis, Structure, Properties and Applications*; Jorio, A., Dresselhaus, G., Dresselhaus, M. S., Eds.; Springer: Berlin, 2008; pp 13−62.
(3) Jena, D. Graphene. In *Encyclopedia of Nanotechnology*; Bhushan, B., Ed.; Springer: Dordrecht, The Netherlands, 2012; pp 968−978.
(4) Lee, C.; Wei, X. D.; Kysar, J. W.; Hone, J. Measurement of the elastic properties and intrinsic strength of monolayer graphene. *Science* **2008**, *321*, 385−388.
(5) Poot, M.; van der Zant, H. S. J. Nanomechanical properties of few-layer graphene membranes. *Appl. Phys. Lett.* **2008**, *92*, 063111.
(6) Vijayaraghavan, A. Graphene—Properties and Characterization. In *Springer Handbook of Nanomaterials*; Vajtai, R., Ed.; Springer: Berlin, 2013; pp 39−82, DOI: 10.1007/978-3-642-20595-8_2.
(7) Balandin, A. A.; Ghosh, S.; Bao, W.; Calizo, I.; Teweldebrhan, D.; Miao, F.; Lau, C. N. Superior thermal conductivity of single-layer graphene. *Nano Lett.* **2008**, *8* (3), 902−907.
(8) Sukhadolau, A. V.; Ivakin, E. V.; Ralchenko, V. G.; Khomich, A. V.; Vlasov, A. V.; Popovich, A. F. Thermal conductivity of CVD diamond at elevated temperatures. *Diamond Relat. Mater.* **2005**, *14*, 589−593.
(9) Allen, M. J.; Tung, V. C.; Kaner, R. B. Honeycomb carbon: A review of graphene. *Chem. Rev.* **2010**, *110*, 132−145.
(10) Novoselov, K. S.; Geim, A. K.; Morozov, S. V.; Jiang, D.; Katsnelson, M. I.; Grigorieva, I. V.; Dubonos, S. V.; Firsov, A. A. Two-dimensional gas of massless Dirac fermions in graphene. *Nature* **2005**, *438*, 197−200.
(11) Zhang, Y. B.; Tan, Y. W.; Stormer, H. L.; Kim, P. Experimental observation of the quantum Hall effect and Berry's phase in graphene. *Nature* **2005**, *438*, 201−204.
(12) Li, X. S.; Cai, W. W.; An, J. H.; Kim, S.; Nah, J.; Yang, D. X.; Piner, R.; Velamakanni, A.; Jung, I.; Tutuc, E.; Banerjee, S. K.; Colombo, L.; Ruoff, R. S. Large-Area Synthesis of High-Quality and Uniform Graphene Films on Copper Foils. *Science* **2009**, *324*, 1312−1314.
(13) Avouris, P.; Dimitrakopoulos, C. Graphene: synthesis and applications. *Mater. Today* **2012**, *15*, 86−97.
(14) Pei, S.; Cheng, H.-M. The reduction of graphene oxide. *Carbon* **2012**, *50*, 3210−3228.
(15) Brodie, B. C. On the Atomic Weight of Graphite. *Philos. Trans. R. Soc. Lond* **1859**, *149*, 249−259.
(16) Staudenmaier, L. Verfahren zur Darstellung der Graphitsäure. *Ber. Dtsch. Chem. Ges.* **1898**, *31*, 1481−1487.

DOI: 10.1021/acs.chemmater.7b01438
Chem. Mater. 2017, 29, 6698−6705

(17) Hofmann, U.; Frenzel, A. Die Reduktion von Graphitoxyd mit Schwefelwasserstoff. *Colloid Polym. Sci.* **1934**, *68*, 149−151.
(18) Hummers, W. S.; Offeman, R. E. Preparation of Graphitic Oxide. *J. Am. Chem. Soc.* **1958**, *80*, 1339−1339.
(19) Marcano, D. C.; Kosynkin, D. V.; Berlin, J. M.; Sinitskii, A.; Sun, Z.; Slesarev, A.; Alemany, L. B.; Lu, W.; Tour, J. M. Improved Synthesis of Graphene Oxide. *ACS Nano* **2010**, *4*, 4806−4814.
(20) Jankovský, O.; Marvan, P.; Nováček, M.; Luxa, J.; Mazánek, V.; Klímová, K.; Sedmidubský, D.; Sofer, Z. Synthesis procedure and type of graphite oxide strongly influence resulting graphene properties. *Appl. Mater. Today* **2016**, *4*, 45−53.
(21) Botas, C.; Álvarez, P.; Blanco, P.; Granda, M.; Blanco, C.; Santamaría, R.; Romasanta, L. J.; Verdejo, R.; López-Manchado, M. A.; Menéndez, R. Graphene materials with different structures prepared from the same graphite by the Hummers and Brodie methods. *Carbon* **2013**, *65*, 156−164.
(22) Chua, C. K.; Pumera, M. Chemical reduction of graphene oxide: a synthetic chemistry viewpoint. *Chem. Soc. Rev.* **2014**, *43*, 291−312.
(23) Sadasivuni, K. K.; Ponnamma, D.; Thomas, S.; Grohens, Y. Evolution from graphite to graphene elastomer composites. *Prog. Polym. Sci.* **2014**, *39*, 749−780.
(24) Haubner, K.; Murawski, J.; Olk, P.; Eng, L. M.; Ziegler, C.; Adolphi, B.; Jaehne, E. The Route to Functional Graphene Oxide. *ChemPhysChem* **2010**, *11*, 2131−2139.
(25) Chen, C. M.; Zhang, Q.; Zhao, X. C.; Zhang, B.; Kong, Q. Q.; Yang, M. G.; Yang, Q. H.; Wang, M. Z.; Yang, Y. G.; Schlögl, R.; Su, D. S. Hierarchically aminated graphene honeycombs for electrochemical capacitive energy storage. *J. Mater. Chem.* **2012**, *22*, 14076−14084.
(26) Kumar, R.; Agrawal, A.; Nagarale, R. K.; Sharma, A. High Performance Supercapacitors from Novel Metal-Doped Ceria Decorated Aminated Graphene. *J. Phys. Chem. C* **2016**, *120*, 3107−3116.
(27) Liu, Z.; Robinson, T. J.; Sun, X.; Dai, H. PEGylated Nanographene Oxide for Delivery of Water-Insoluble Cancer Drugs. *J. Am. Chem. Soc.* **2008**, *130*, 10876−10877.
(28) Valentini, L.; Cardinali, M.; Bittolo Bon, S.; Bagnis, D.; Verdejo, R.; Lopez-Manchado, M. A.; Kenny, J. M. Use of butylamine modified graphene sheets in polymer solar cells. *J. Mater. Chem.* **2010**, *20*, 995−1000.
(29) Wang, B.; Luo, B.; Liang, M.; Wang, A.; Wang, J.; Fang, Y.; Chang, Y.; Zhi, L. Chemical amination of graphene oxides and their extraordinary properties in the detection of lead ions. *Nanoscale* **2011**, *3*, 5059−5066.
(30) Qin, H.; Hwang, T.; Ahn, C.; Kim, J. A.; Jin, Y.; Cho, Y.; Shin, C.; Kim, T. Chemical Amination via Cycloaddition of Graphene for Use in a Glucose Sensor. *J. Nanosci. Nanotechnol.* **2016**, *16*, 5034−5037.
(31) Zhang, W.; Ma, J.; Gao, D.; Zhou, Y.; Li, C.; Zha, J.; Zhang, J. Preparation of amino-functionalized graphene oxide by Hoffman rearrangement and its performances on polyacrylate coating latex. *Prog. Org. Coat.* **2016**, *94*, 9−17.
(32) Gong, X.; Liu, G.; Li, Y.; Yu, D. Y. W.; Teoh, W. Y. Functionalized-Graphene Composites: Fabrication and Applications in Sustainable Energy and Environment. *Chem. Mater.* **2016**, *28*, 8082−8118.
(33) Bourlinos, A. B.; Gournis, D.; Petridis, D.; Szabó, T.; Szeri, A.; Dékány, I. Graphite Oxide: Chemical Reduction to Graphite and Surface Modification with Primary Aliphatic Amines and Amino Acids. *Langmuir* **2003**, *19*, 6050−6055.
(34) Bittolo Bon, S.; Valentini, L.; Verdejo, R.; Garcia Fierro, J. L.; Peponi, L.; Lopez-Manchado, M. A.; Kenny, J. M. Plasma Fluorination of Chemically Derived Graphene Sheets and Subsequent Modification with Butylamine. *Chem. Mater.* **2009**, *21*, 3433−3438.
(35) Lai, L.; Chen, L.; Zhan, D.; Sun, L.; Liu, J.; Lim, S. H.; Poh, C. K.; Shen, Z.; Lin, J. One-step synthesis of NH_2-graphene from in situ graphene-oxide reduction and its improved electrochemical properties. *Carbon* **2011**, *49*, 3250−3257.
(36) Li, X.; Wang, H.; Robinson, J. T.; Sanchez, H.; Diankov, G.; Dai, H. Simultaneous Nitrogen Doping and Reduction of Graphene Oxide. *J. Am. Chem. Soc.* **2009**, *131*, 15939−15944.
(37) Jiang, B.; Tian, C.; Wang, L.; Sun, L.; Chen, C.; Nong, X.; Qiao, Y.; Fu, H. Highly concentrated, stable nitrogen-doped graphene for supercapacitors: Simultaneous doping and reduction. *Appl. Surf. Sci.* **2012**, *258*, 3438−3443.
(38) Chen, P.; Yang, J.-J.; Li, S.-S.; Wang, Z.; Xiao, T.-Y.; Qian, Y.-H.; Yu, S.-H. Hydrothermal synthesis of macroscopic nitrogen-doped graphene hydrogels for ultrafast supercapacitor. *Nano Energy* **2013**, *2*, 249−256.
(39) Sun, L.; Wang, L.; Tian, C. G.; Tan, T. X.; Xie, Y.; Shi, K. Y.; Li, M. T.; Fu, H. G. Nitrogen-doped graphene with high nitrogen level via a one-step hydrothermal reaction of graphene oxide with urea for superior capacitive energy storage. *RSC Adv.* **2012**, *2*, 4498−4506.
(40) Su, P.; Guo, H.-L.; Peng, S.; Ning, S.-K. Preparation of Nitrogen-Doped Graphene and Its Supercapacitive Properties. *Acta Phys.-Chim. Sin.* **2012**, *28*, 2745−2753.
(41) Guo, H.-L.; Su, P.; Kang, X.; Ning, S.-K. Synthesis and characterization of nitrogen-doped graphene hydrogels by hydrothermal route with urea as reducing-doping agents. *J. Mater. Chem. A* **2013**, *1*, 2248−2255.
(42) Long, D.; Li, W.; Ling, L.; Miyawaki, J.; Mochida, I.; Yoon, S.-H. Preparation of Nitrogen-Doped Graphene Sheets by a Combined Chemical and Hydrothermal Reduction of Graphene Oxide. *Langmuir* **2010**, *26*, 16096−16102.
(43) Lee, J. W.; Ko, J. M.; Kim, J.-D. Hydrothermal preparation of nitrogen-doped graphene sheets via hexamethylenetetramine for application as supercapacitor electrodes. *Electrochim. Acta* **2012**, *85*, 459−466.
(44) Leuckart, R. Ueber eine neue Bildungsweise von Tribenzylamin. *Ber. Dtsch. Chem. Ges.* **1885**, *18*, 2341−2344.
(45) Leuckart, R.; Bach, E. Ueber die Einwirkung von Ammoniumformiat auf Benzaldehyd und Benzophenon. *Ber. Dtsch. Chem. Ges.* **1886**, *19*, 2128−2131.
(46) Leuckart, R.; Bach, E. Ueber Bornylamin. *Ber. Dtsch. Chem. Ges.* **1887**, *20*, 104−114.
(47) Leuckart, R.; Janssen, H. Ueber die Einwirkung von Ammoniumformiat auf Desoxybenzoïn. Symmetrisches Diphenyläthylamin. *Ber. Dtsch. Chem. Ges.* **1889**, *22*, 1409−1413.
(48) Viezbicke, B.; Patel, S.; Davis, B.; Birnie, D., III Evaluation of the Tauc method for optical absorption edge determination: ZnO thin films as a model system. *Phys. Status Solidi B* **2015**, *252*, 1700−1710.
(49) Lee, D. W.; De Los Santos V, L.; Seo, J. W.; Felix, L. L.; Bustamante D, A.; Cole, J. M.; Barnes, C. H. W. The Structure of Graphite Oxide: Investigation of Its Surface Chemical Groups. *J. Phys. Chem. B* **2010**, *114*, 5723−5728.
(50) Rubtsov, I. V.; Wang, J.; Hochstrasser, R. M. Vibrational coupling between amide-I and amide-A modes revealed by femtosecond two color infrared spectroscopy. *J. Phys. Chem. A* **2003**, *107*, 3384−3396.
(51) Kline, C. H., Jr.; Turkevich, J. The vibrational spectrum of pyridine and the thermodynamic properties of pyridine vapors. *J. Chem. Phys.* **1944**, *12*, 300−309.
(52) Zhang, Y.; Sun, Z.; Wang, H.; Wang, Y.; Liang, M.; Xue, S. Nitrogen-doped graphene as a cathode material for dye-sensitized solar cells: effects of hydrothermal reaction and annealing on electrocatalytic performance. *RSC Adv.* **2015**, *5*, 10430−10439.
(53) Lou, F.; Buan, M. E. M.; Muthuswamy, N.; Walmsley, J. C.; Ronning, M.; Chen, D. One-step electrochemical synthesis of tunable nitrogen-doped graphene. *J. Mater. Chem. A* **2016**, *4*, 1233−1243.
(54) Xue, Q.; Sun, J. Electrical Conductivity and Percolation Behavior of Polymer Nanocomposites. In *Polymer Nanocomposites: Electrical and Thermal Properties*; Huang, X., Zhi, C., Eds.; Springer: Cham, Switzerland, 2016; pp 51−82, DOI: 10.1007/978-3-319-28238-1_3.
(55) Shang, Y.; Xu, H.; Li, M.; Zhang, G. Preparation of N-Doped Graphene by Hydrothermal Method and Interpretation of N-Doped Mechanism. *Nano* **2017**, *12*, 1750018.

DOI: 10.1021/acs.chemmater.7b01438
Chem. Mater. 2017, 29, 6698−6705

(56) Navaee, A.; Salimi, A. Efficient amine functionalization of graphene oxide through the Bucherer reaction: an extraordinary metal-free electrocatalyst for the oxygen reduction reaction. *RSC Adv.* **2015**, *5*, 59874−59880.
(57) Ferrari, A. C.; Basko, D. M. Raman spectroscopy as a versatile tool for studying the properties of grafene. *Nat. Nanotechnol.* **2013**, *8*, 235−246.
(58) Pimenta, M. A.; Dresselhaus, G.; Dresselhaus, M. S.; Cançado, L. G.; Jorio, A.; Saito, R. Studying disorder in graphite-based systems by Raman spectroscopy. *Phys. Chem. Chem. Phys.* **2007**, *9*, 1276−1291.
(59) Rani, P.; Jindal, V. K. Designing band gap of graphene by B and N dopant atoms. *RSC Adv.* **2013**, *3*, 802−812.
(60) Botas, C.; Álvarez, P.; Blanco, C.; Santamaría, R.; Granda, M.; Gutiérrez, M. D.; Rodríguez-Reinoso, F.; Menéndez, R. Critical temperatures in the synthesis of graphene-like materials by thermal exfoliation−reduction of graphite oxide. *Carbon* **2013**, *52*, 476−485.
(61) Jansen, R. J. J.; van Bekkum, H. XPS of nitrogen-containing functional groups on activated carbon. *Carbon* **1995**, *33*, 1021−1027.
(62) Crumpton, D. M.; Laitinen, R. A.; Smieja, J.; Cleary, D. A. Thermal Analysis of Carbon Allotropes: An Experiment for Advanced Undergraduates. *J. Chem. Educ.* **1996**, *73*, 590−591.
(63) Arndt, F. G.; Coggeshall, N. D.; Dal Nogare, S.; Elek, A.; Jungnickel, J. L.; Mehlenbacher, V. C.; Mitchell, J.; Peters, E. D.; Polgár, A.; Weiss, F. T.; Wright, G. F. In *Organic analysis*, Vol. *I*; Mitchell, J., Kolthoff, I. M., Proskauer, E. S., Weissberger, A., Eds.; Interscience: New York, London, 1954; pp 302−304.
(64) Weiss, J. *Handbook of Ion Chromatography*, 3rd ed.; Wiley-VCH Verlag; Darmstadt, Germany, 2004; pp 389−392.
(65) Kaniyoor, A.; Baby, T. T.; Arockiadoss, T.; Rajalakshmi, N.; Ramaprabhu, S. Wrinkled Graphenes: A Study on the Effects of Synthesis Parameters on Exfoliation-Reduction of Graphite Oxide. *J. Phys. Chem. C* **2011**, *115*, 17660−17669.
(66) Paredes, J. I.; Villar-Rodil, S.; Martínez-Alonso, A.; Tascón, J. M. D. Graphene Oxide Dispersions in Organic Solvents. *Langmuir* **2008**, *24*, 10560−10564.
(67) Wallace, P. R. The band Theory of Graphite. *Phys. Rev.* **1947**, *71*, 622−634.
(68) Hsu, H.-C.; Shown, I.; Wei, H.-Y.; Chang, Y.-C.; Du, H.-Y.; Lin, Y.-G.; Tseng, C.-A.; Wang, C.-H.; Chen, L.-C.; Lin, Y.-C.; Chen, K.-H. Graphene oxide as a promising photocatalyst for CO2 to methanol conversion. *Nanoscale* **2013**, *5*, 262−268.
(69) Velasco-Soto, M. A.; Pérez-García, S. A.; Alvarez-Quintana, J.; Cao, Y.; Nyborg, L.; Licea-Jiménez, L. Selective band gap manipulation of graphene oxide by its reduction with mild reagents. *Carbon* **2015**, *93*, 967−973.
(70) Crossley, F. S.; Moore, M. L. Studies on the leuckart reaction. *J. Org. Chem.* **1944**, *9*, 529−536.
(71) Moore, M. L. The Leuckart Reaction. *Organic Reactions*; John Wiley & Sons: New York, *2011*; pp 301−330, DOI: 10.1002/0471264180.or005.07.

DOI: 10.1021/acs.chemmater.7b01438
Chem. Mater. 2017, 29, 6698−6705